Self-vacancies in gallium arsenide: An *ab initio* calculation

Fedwa El-Mellouhi* and Normand Mousseau†
Département de Physique and Regroupement Québécois sur les Matériaux de Pointe, Université de Montréal, Case postale 6128, succursale Centre-ville, Montréal (Québec) H3C 3J7, Canada
(Received 9 September 2004; revised manuscript received 7 December 2004; published 18 March 2005)

We report here a reexamination of the static properties of vacancies in GaAs by means of first-principles density-functional calculations using localized basis sets. Our calculated formation energies yields results that are in good agreement with recent experimental and *ab initio* calculation and provide a complete description of the relaxation geometry and energetic for various charge states of vacancies from both sublattices. Gallium vacancies are stable in the 0, −, −2, −3 charge states, but V_{Ga}^{-3} remains the dominant charge state for intrinsic and *n*-type GaAs, confirming results from positron annihilation. Interestingly, arsenic vacancies show two successive negative-*U* transitions making only +1, −1, and −3 charge states stable, while the intermediate defects are metastable. The second transition (−/−3) brings a resonant bond relaxation for V_{As}^{-3} similar to the one identified for silicon and GaAs divacancies.

DOI: 10.1103/PhysRevB.71.125207 PACS number(s): 71.15.Pd, 61.72.Ji, 71.15.Mb

I. INTRODUCTION

Native point defects are involved in virtually every process during which an atom incorporated in the lattice of a semiconductor migrates toward another lattice site. This diffusion mediated by point defects is responsible for a number of important effects, for instance, those encountered during fabrication of microelectronic devices. It is not surprising therefore that point defects in semiconductors have been extensively studied using *ab initio* techniques. Some work still remains to be done, however, especially in the case of alloyed semiconductors.

If Ga vacancies in GaAs are relatively well understood—because most dopants used in technology (Si donor, Zn, Be, and Mg acceptors) occupy the Ga sites—much less is known about the As vacancy. The recent introduction of carbon as a prospective As-site acceptor has raised significantly the interest for this defect,[1] however. There is therefore abundant literature on calculations[1–10] of formation energies of point defects in GaAs which is nicely reviewed and summarized in a paper of Deepak *et al.*[11] Since formation energies are difficult to measure, calculations are the primary method for obtaining these values. However, because of the assumptions and approximations taken into account, the reported values in the literature during the last two decades differ greatly from paper to paper.

Most calculations were done for small supercells. These calculations take advantage of error cancellations to obtain energy differences that are more precise than the total energies themselves. Here we repeat these calculations for all possible charge states for both Ga and As vacancies using the strict convergence criteria and a large simulation cell.

The outline of the paper is as follows. We first describe the method for defect calculation in Sec. II, then we turn to the convergence tests made to set up the methodology. We focus on the effect of the *k*-point sampling, system size, and completeness of the basis on the formation energy and structural properties of the defects. Section III deals with these effects on the most important charge states such as V_{As}^{-1} and V_{Ga}^{-3}. In Sec. IV we present and discuss the most converged results using localized basis sets compared to previous results obtained from theory and experiment.

II. SIMULATION DETAILS AND METHODOLOGY

A. Total energy calculations

The total energies for this work are evaluated using SIESTA,[12,13] a self-consistent density functional method (DFT) within local-density approximation (LDA). Core electrons are represented by the standard norm-conserving Troullier-Martins pseudopotentials[14] factorized in the Kleiman-Baylander form[15] and the one-particle problem is solved using linear combination of pseudoatomic orbitals (PAO) basis set of finite range. These orbitals are strictly localized and represent well the local electronic densities; few of them are therefore needed, decreasing considerably the computational costs by comparison with standard plane-waves calculations. The main drawback of this approach, however, is the lack of a systematic procedure to ensure a rapid variational convergence with respect to the number of basis orbitals and to the range and shape of each orbital. Consequently, while extending plane-wave basis sets is trivial, some efforts are needed to prepare unbiased pseudoatomic basis sets (see, for example, Refs. 16 and 17).

In this work, we use the following sequence to test the convergence of the basis set. Starting with the simplest scheme, a single ζ (SZ) basis, a second group of valence orbitals is added for flexibility, forming the double-ζ (DZ) basis. For completeness, we also add polarization orbitals to both valence sets, generating SZP and DZP bases.

Finally, it is possible to optimize the localization radius in order to increase the accuracy for a given basis set. While the computational efficiency is slightly reduced, as the optimized orbitals have generally a longer tail, it is often a good alternative to increase the size of the basis set (for details see Refs. 12–14). We also test the accuracy of these basis sets optimized with respect to the amount of overlap between

 ©2005 The American Physical Society

TABLE I. Comparison between converged basic parameters for bulk GaAs. a, B, and E_{total} represent the lattice constant (Å), the bulk modulus (GPa), and the total energy per GaAs pair (eV/pair), respectively. E_g denotes the energy gap (eV) and ΔH is the heat of formation of GaAs calculated using Eq. (4) (eV). See the text for description of the basis set label. Results are compared to a recent plane-wave (PW) calculation (Ref. 18) and to experimental values from Ref. 19 at 0 K, unless other references are cited.

	SZ	SZ-O	SZP-O	DZ	DZP	PW	Expt.
a	5.68	5.66	5.60	5.64	5.60	5.55	5.65
B	59.3	68.9	78.8	67.7	70.4		75.3
E_{total}	235.2	235.5	235.9	235.7	236.0		
E_g	0.61	0.78	0.98	0.66	0.82	1.08[a]	1.52
						0.7[b]	
ΔH	0.66	0.99	0.78	0.81	0.72	1.0[a]	0.73[e]
						0.67[c]	
						0.83[d]	

[a]Reference 18.
[b]Reference 3.
[c]Reference 8.
[d]Reference 1.
[e]Reference 20.

atomic orbitals around the defect using the optimizing procedure of Anglada *et al.*[17] at 0.0 GPa for the SZ basis set. We find that the efficiency of these orbitals with (SZP-O) and with (SZ-O) is comparable to those of DZP and DZ, respectively.

Table I reports the values of a number of structural and thermodynamical quantities for bulk GaAs as computed using these various bases with a k-point sampling density of 0.03 Å^{-1}, corresponding to that for a 216-atom unit cell with a $2\times2\times2$ k-point sampling. For SZ, the lattice constant at zero pressure is found to be 5.68 Å, overestimating the experimental value by only 0.03 Å. The density of the GaAs crystal increases with the size of the basis set, and the lattice constant for DZP is found to be too small by 0.05 Å with respect to experiment. The relatively contracted structure obtained with DZP is characteristic of LDA; plane-wave calculations also using LDA give 5.55 Å.[18] Increasing the basis set leads to a significant improvement on the calculated value of the bulk modulus as it goes from 59.85 GPa for SZ to 70.4 GPa for DZP, close to the experimental value of 75.3 GPa.

The LDA band gap is found to be 0.61, 0.66, and 0.82 eV for SZ, DZ, and DZP basis sets, respectively, underestimating, as usual with this approximation, the experimental gap of 1.52 eV. The DZP band gap lies well within the range of energy gaps obtained from PW (0.7–1.1 eV),[3,18] however, and can be considered converged.

No such systematic problem is found for the total energy and the heat of formation. In particular, the heat of formation obtained with DZ and DZP is very close to the experimental value,[20] showing a better agreement than previous plane-waves calculations.[1,8,18]

Overall, therefore, we see a well-defined trend in the structural and thermodynamical values shown in Table I: most quantities converge rapidly as the basis goes from SZ to DZ to DZP, with DZP providing an excellent agreement with experiment. Moreover, it appears that the optimal basis sets, SZ-O and SZP-O, compare very well with DZP, suggesting that they could be used when computational costs are an issue. The application of these optimized bases to study the diffusion of vacancies in GaAs will be reported somewhere else.[21]

B. Defects formation energies in supercell calculations

When computing structural and energetic properties of defects using *ab initio* methods, it is important to ensure that the size of the basis set is complete enough but also that the simulation cell is sufficiently large to avoid self-interaction between the defect and its images. We have shown previously,[22] in a study of the neutral vacancy in silicon, that a cubic supercell of at least 216 atomic sites can be necessary in order to reduce the elastic and electronic self-interaction and obtain the right symmetry around the defect.[23] As discussed in Sec. IV B 1, we find a similar behavior for As vacancy; unless indicated, therefore, we use a 215-atom cell for all our calculations of defects.

In all calculations, this initial 215-atom configuration cell is randomly distorted, to avoid imposing spurious symmetry in the fully relaxed defect state. All atoms are allowed to relax without any constraint until every force component falls below 0.04 eV/Å. The energy minimization takes place at a constant volume, using the optimal lattice constant obtained with DZP, 5.6 Å (see Table I), 1% denser than the experimental value.

The formation energy can be evaluated directly from total energies obtained from electronic structure calculations. For binary compounds it is current to use the formalism of Zhang and Northrup[2] (see Ref. 24 for intermediate steps). The formation energy of a defect of charge state q is defined as

$$E_f = E'_f + q(E_V + \mu_e) - \frac{1}{2}(n_{\text{As}} - n_{\text{Ga}})\Delta\mu, \qquad (1)$$

where E'_f is independent of $\Delta\mu$ and μ_e, and is represented by

$$E'_f = E_{\text{tot}}(q) - \frac{1}{2}(n_{\text{As}} + n_{\text{Ga}})\mu^{\text{bulk}}_{\text{GaAs}} - \frac{1}{2}(n_{\text{As}} - n_{\text{Ga}})(\mu^{\text{bulk}}_{\text{As}} - \mu^{\text{bulk}}_{\text{Ga}}), \qquad (2)$$

where n_{As} and n_{Ga} are the number of As and Ga ions present in the sample, q denotes the net number of electrons or holes supported by the vacancy, μ_e is the electron chemical potential or the Fermi energy E_F, and E_V is the energy at the valence band maximum. Errors in E_V due to the finite supercell are corrected by aligning the vacuum levels of the defective supercell and undefected supercell.[25]

If $\Delta\mu$ is defined as the chemical potential difference

$$\Delta\mu = (\mu_{\text{As}} - \mu_{\text{Ga}}) - (\mu^{\text{bulk}}_{\text{As}} - \mu^{\text{bulk}}_{\text{Ga}}), \qquad (3)$$

the restriction on the chemical potentials becomes $0 \leqslant \mu_e \leqslant E_g$ and $-\Delta H \leqslant \Delta\mu \leqslant \Delta H$, where E_g is the energy

gap, and the heat of formation ΔH of bulk GaAs is defined as the difference between the chemical potential of bulk As and bulk Ga crystals and that of bulk GaAs. This latter quantity represents the energy necessary to dissociate GaAs into its individual components

$$\Delta H = \mu_{\mathrm{As}}^{\mathrm{bulk}} + \mu_{\mathrm{Ga}}^{\mathrm{bulk}} - \mu_{\mathrm{GaAs}}^{\mathrm{bulk}}. \quad (4)$$

For Ga vacancies of charge q the Eq. (1) reduces to

$$E_f = E_f' + q(E_V + \mu_e) - \frac{1}{2}\Delta\mu \quad (5)$$

with $E_f' = E_{\mathrm{tot}}(q) - \frac{215}{2}\mu_{\mathrm{GaAs}}^{\mathrm{bulk}} + \frac{1}{2}(\mu_{\mathrm{As}}^{\mathrm{bulk}} - \mu_{\mathrm{Ga}}^{\mathrm{bulk}})$; for As vacancies, it becomes

$$E_f = E_f' + q(E_V + \mu_e) + \frac{1}{2}\Delta\mu \quad (6)$$

and $E_f' = E_{\mathrm{tot}}(q) - \frac{215}{2}\mu_{\mathrm{GaAs}}^{\mathrm{bulk}} - \frac{1}{2}(\mu_{\mathrm{As}}^{\mathrm{bulk}} - \mu_{\mathrm{Ga}}^{\mathrm{bulk}})$.

C. Computing the ionization energy of charged defects

The concentration of charged defects is controlled by the position of the Fermi level which is determined by the local concentration of carriers. Since GaAs is used in a doped state in devices, it is important to assess the possible charged states of defects.

Charges can affect strongly the formation energy as well as the structure of a defect, changing the symmetry of the relaxed state and altering considerably the local electronic properties. For charged defects, the effects of a finite-size supercell will be even more marked due to the long-ranged nature of the Coulomb interaction; the use of a sufficiently large supercell is therefore even more important.

To account for the electrostatic interaction of periodically arranged defects of charge q as well as their interaction with the compensating background, we follow the approximate procedure of Makov and Payne.[26] The correction to the total energy of a charged system is handled by SIESTA, and it consists of a monopole correction only ($q^2\alpha/2\varepsilon L$), where α is the Madelung constant of the simple cubic lattice, L is the defect-defect distance (16.8 Å), and ε is the experimental static dielectric constant. The monopole correction is found to be 0.094, 0.37, and 0.84 eV for the charge states ±1, ±2, and ±3, respectively. The quadrupole correction, which we evaluated by hand, is proportional to $1/L^3$. For the 215-atom supercell, it is $2.42\times 10^{-6} qQ$ eV (where Q is the quadrupole moment), and can therefore be neglected (see also Refs. 27 and 28).

Because of the limitations of LDA, localized DFT eigenvalues are not equivalent to the measured electronic levels. Thus ionization energy is obtained from the difference between q_1 and q_2 electron total energy calculations $[\epsilon(q_2/q_1) = E_{\mathrm{tot}}^{q_1} - E_{\mathrm{tot}}^{q_2} - (q2-q1)E_V]$, rather than the difference of q_2 and q_1 electron eigenvalues of a single calculation. Usually only one electron is transferred between the electron reservoir and the defect levels. When two electrons are transferred at the same time the electron-electron repulsion is compensated by a relaxation of the structure around the defect that arises from a strong electron-phonon coupling. This so-called "negative-U effect" is found when the ionization level $\epsilon[(q-1)/q]$ appears above $\epsilon[q/(q+1)]$, thus a direct transition $[(q-1)/(q+1)]$ is energetically more favorable.[29]

III. CONVERGING DEFECT FORMATION AND IONIZATION ENERGIES

In this section, we study the effects of the basis set, the k sampling, and the simulation cell size on the formation energy and the relaxed geometry of neutral and charged Ga and As vacancies. A special emphasis is put on V_{Ga}^{-3} and V_{As}^{+1} for the analysis of convergence. These are the dominant charge states as is discussed in Sec. IV.

A. Local basis set effect

We first study the effect of the choice of the local basis set on the defects. In order to cancel out all other effects, we use supercells of 215 atomic sites and a Monkhorst-Pack grid[30] of $2\times 2\times 2$ corresponding to a density of 0.03 Å^{-1} of k points.

Cohesive energies as well as bulk moduli studied in Sec. II A for the different basis sets used show that atomic bonding is strengthened progressively as we go from SZ basis to DZP. Structural relaxation is directly related to the interatomic forces acting on atoms around the vacancy and on the strength of atomic bonding. Atoms around the vacancy form initially an ideal tetrahedron with six equal distances labeled d_1–d_6 with tetrahedral symmetry T_d. After the full relaxation (see Sec. II A), distances and angles can be altered and the symmetry is either conserved or broken.

Relaxations around the vacancies are given for different charge states in Tables II and III for Ga and As vacancies, respectively. In both cases the corresponding formation energy is reported as well as the relative change in the volume of the tetrahedron with respect to the ideal one.[23,24]

Due to the finite precision in the relaxation, there is some imprecision in the identification of the defect symmetry. Here, if the highest relative difference between two bonds is lower than 1% (equivalent to a precision of 0.04 Å), the structure is assigned to the highest symmetry group. The last column lists the symmetry groups for the different defects in the DZP basis set. Unless specified, the symmetry group for all bases is the same as that of DZP.

1. V_{Ga}

The Ga vacancy maintains the same symmetry for all charge states irrespective of the basis set used. The structural relaxation is most important for the smallest basis set, SZ, decreasing progressively by about one third as the number of orbitals is increased, but the T_d symmetry is maintained in all cases, with the atoms moving inwards systematically. Moreover, for each basis set the degree of structural relaxation is almost independent of the charge state, the variation of the structural relaxation from the neutral to the −3 charge state goes from 2% (SZ) to 8% (DZP). As can be seen in Table II, the formation energy is also rather well converged with the minimal basis set (SZ), by comparison with the more accu-

TABLE II. Convergence of the formation energy E_f' in eV with respect to the basis set for the Ga vacancy. Relaxation around the vacancy are given in % compared to the ideal tetrahedral distance between As nearest neighbors (most converged results are shown in bold). The distances are labeled $d_1 - d_6$, the negative sign indicates an inward relaxation. The tetrahedron volume change is also given in % of the ideal volume $[\Delta V = 100(V - V_0)/V_0]$. The last column displays the symmetry group of the defect (see the text for more details).

Basis	E_f' (eV)	Distances in % d_1	d_2	d_3	d_4	d_5	d_6	ΔV	Symmetry
				V_{Ga}^{0}					
SZ	2.7	−19.3	−19.2	−19.3	−19.3	−19.2	−19.3	−47.3	
DZ	2.8	−14.5	−14.4	−14.5	−14.4	−14.5	−14.4	−37.4	
DZP	**2.9**	**−13.5**	**−13.4**	**−13.5**	**−13.4**	**−13.4**	**−13.5**	**−35.2**	T_d
				V_{Ga}^{-1}					
SZ	2.9	−19.0	−19.1	−19.0	−19.0	−19.0	−19.0	−46.9	
DZ	2.9	−14.7	−14.7	−14.7	−14.7	−14.7	−14.7	−37.9	
DZP	**3.0**	**−14.2**	**−14.2**	**−14.2**	**−14.2**	**−14.2**	**−14.2**	**−36.9**	T_d
				V_{Ga}^{-2}					
SZ	3.4	−19.5	−19.5	−19.5	−19.5	−19.5	−19.5	−47.8	
DZ	3.2	−14.4	−14.4	−14.4	−14.4	−14.4	−14.4	−37.3	
DZP	**3.4**	**−14.0**	**−14.1**	**−14.0**	**−14.0**	**−14.1**	**−14.0**	**−36.5**	T_d
				V_{Ga}^{-3}					
SZ	4.1	−19.7	−19.8	−19.7	−19.7	−19.8	−19.7	−48.3	
DZ	3.8	−15.1	−15.2	−15.1	−15.1	−15.2	−15.1	−38.9	
DZP	**3.9**	**−14.6**	**−14.6**	**−14.6**	**−14.6**	**−14.7**	**−14.6**	**−37.7**	T_d

rate DZP: the difference between the two bases is at most 0.2 eV.

Heavily charged defects such as V_{Ga}^{-3}, which is the most likely charge state in a heavily doped material, are more sensitive to the completeness of the basis set. This effect explains the fact that the formation energy decreases with an improved basis, contrary to the other defects.

Because of its technological importance, we must ensure that the orbital overlap around the vacant site is sufficient to accommodate the extra electrons in V_{Ga}^{-3}. We can do so by placing a *ghost* Ga atom at the defect site. For that purpose, we generate a set of orbitals and place them on the crystalline site, without adding any pseudopotential or extra electrons. The system is then relaxed using the same convergence criterion as before. This ghost atom does not have any significant effect on the total energy of the defect when the DZ and the DZP basis sets are used. In contrast, SZ basis total energies are corrected by 0.34 eV, suggesting that the SZ orbitals are too short. This additional set of orbitals is sufficient to correct for the overestimated formation energy with SZ basis, decreasing its value from 4.06 to 3.72 eV, following the general trend observed for other charge states (see Table II).

2. V_{As}

The situation is very different for the As vacancy: the local symmetry is broken for most charge states and the completeness of the basis set impacts strongly on the reconstruction around the defect. Except for the positively charged vacancy, the bonds are stretched considerably to form pairs, leading to volume deformation by as much as 60%. Because of this strong deformation, we relax the threshold condition on the relative difference between two bonds used to determine the symmetry. To allow the reader to judge the impact of a relaxed classification, the distances d_1-d_6 are also indicated (in ascendant order) in Table III.

As a general trend, the SZ basis is less efficient for As than for Ga vacancies: the formation energy is underestimated by as much as 0.6 eV (21%) for charge +1 and 1.0 eV (17%) for charges −3 as compared with DZP. The underestimation drops to 2–8% with DZ, a considerable improvement, for all charge states. The improvement in formation energy can be directly correlated with the prediction quality of the local relaxation. For example, while T_d symmetry is conserved for the three basis sets for V_{As}^{+1}, the change in the volume around the V_{As}^{+1} is highly overestimated by 131% using SZ basis compared to the DZP results. The overestimation drops to 33% with DZ, leading to an error of less than 0.1 eV compared with DZP.

As more electrons are added to the defect level this trend tends to diminish; the symmetry and the relaxation of the defect can be described with reasonable accuracy using the DZ basis. Applied to the singly negative As vacancy V_{As}^{-1}, the inclusion of the ghost atom at the vacant site has a smaller impact on the energy level and relaxation using SZ than for V_{Ga}^{-3}, and next to none with DZ and DZP. For the minimal basis set, the correction is negligible and accounts only for 0.067 eV.

TABLE III. Convergence of the formation energy E_f' in eV with respect to the basis set for the As vacancy. The relaxation around the vacancy is given in % compared to the ideal tetrahedral distance between Ga nearest neighbors (most converged results are shown in bold). The distances are labeled $d_1 - d_6$, the negative sign indicates an inward relaxation. The volume change around the vacancy is also given in % of the ideal volume $[\Delta V = 100(V - V_0)/V_0]$. The last column displays the symmetry group of the defect (see the text for more details).

Basis	E_f' (eV)	Distances in % d_1	d_2	d_3	d_4	d_5	d_6	ΔV	Symmetry
					V_{As}^{+1}				
SZ	2.2	−14.5	−14.9	−15.1	−15.7	−15.9	−16.6	−39.5	
DZ	2.7	−7.9	−8.0	−8.1	−8.4	−8.4	−8.7	−22.7	
DZP	**2.8**	**−5.6**	**−5.9**	**−6.1**	**−6.3**	**−6.2**	**−6.4**	**−17.1**	T_d
					V_{As}^{0}				
SZ	2.4	−13.8	−14.3	−15.2	−15.2	−31.3	−31.7	−53.4	C_{1h}
DZ	3.1	−12.2	−12.2	−12.7	−13.0	−26.9	−27.0	−46.7	$\sim D_{2d}$
DZP	**3.2**	**−11.1**	**−11.2**	**−11.5**	**−11.6**	**−24.6**	**−24.5**	**−43.0**	D_{2d}
					V_{As}^{-1}				
SZ	2.5	−14.3	−14.7	−15.3	−15.4	−33.3	−33.5	−55.6	
DZ	3.2	−12.5	−12.7	−13.2	−13.4	−31.8	−32.0	−52.4	
DZP	**3.3**	**−11.6**	**−11.9**	**−12.5**	**−12.6**	**−31.2**	**−31.5**	**−51.2**	$\sim D_{2d}$
					V_{As}^{-2}				
SZ	3.8	−17.8	−18.5	−18.5	−19.3	−33.6	−33.7	−58.6	$\sim C_{3v}$
DZ	4.4	−16.5	−17.1	−17.5	−18.2	−32.0	−32.3	−56.2	$\sim C_{3v}$
DZP	**4.6**	**−16.5**	**−16.8**	**−17.0**	**−17.6**	**−31.6**	**−31.7**	**−55.4**	C_{3v}/D_{2d}
					V_{As}^{-3}				
SZ	4.9	−18.4	−18.4	−31.4	−31.6	−31.7	−31.8	−65.5	
DZ	5.4	−18.3	−18.2	−30.4	−30.6	−30.7	−31.0	−63.8	
DZP	**5.9**	**−18.1**	**−18.2**	**−30.4**	**−30.2**	**−30.2**	**−30.2**	**−62.9**	D_{2d}-**resonant**

3. Convergence of the ionization energy with the basis sets

As defined in Sec. II C, ionization energies are taken as the difference between the total energy in different charge states, eliminating or decreasing many errors present in the formation energy. For example, errors coming from LDA cancel out and those coming from different chemical potentials are eliminated. The main remaining sources of error are those coming from the basis set convergence, the evaluation of the valence band edge energy, and the Madelung correction.

Figure 1 displays the convergence of the ionization energies as a function of the basis set used for V_{As} and V_{Ga}. For both types of defects, the preliminary results obtained using SZ basis set give a rough estimate of the location of ionization energies in the band gap. These energies converge with increasing basis sets, but slower than the formation energies. For V_{Ga}, while the formation energies are already reasonably converged with the minimal basis set, the ionization levels found using the SZ basis are noticeably overestimated compared to DZP. For V_{As}, we found in Sec. III A 2 that formation energies are underestimated by less than 1 eV with SZ for most charge states. Once ionization energies are calculated, errors on the formation energies coming from the relaxation around the defect cancel out since defects in all charge states suffer from this effect. SZ basis gives a correct qualitative description of the nature of the electronic transition (double negative-U effect, to be discussed in Sec. IV B 1). The location of the levels in the band gap as well as the distance between them are also reasonably converged. Ionization energies with SZ are slightly underestimated compared to the DZP ionization levels.

By studying the effect of the choice of the basis set on the structural relaxation, the formation and the ionization energies, we conclude that the SZ basis is significantly less efficient when the local symmetry is broken. In these cases, the use of a second radial function (DZ) is necessary to obtain reasonable numbers. Moreover, both DZ and DZP are complete enough to represent the properties associated with a defect without the need for a ghost atom.

B. *k*-point effects

The effects of Brillouin zone sampling are studied by comparing the formation energies and the relaxation volume of both As and Ga vacancies for all charge states. We consider two k-point samplings, a Γ-point sampling, and a $2\times2\times2$ Monkhorst-Pack mesh,[30] corresponding, for the 215-atom cell used here, to a density of 0.06 and 0.03 Å^{-1}, respectively. To isolate sampling effects, all calculations are done using the DZP basis set. Results are shown in Table IV.

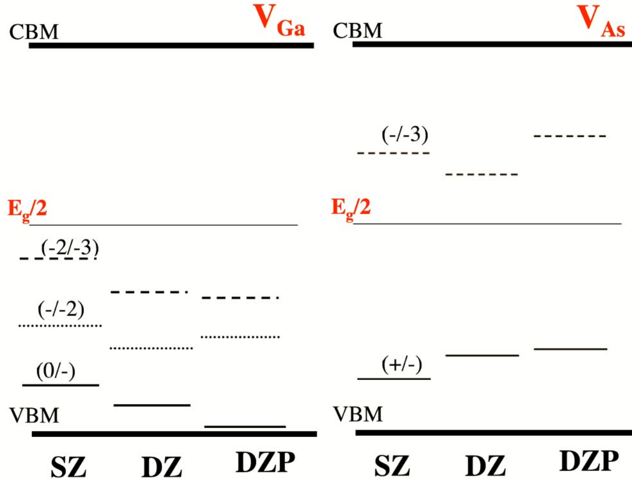

FIG. 1. (Color online) Schematic representation of the convergence of ionization energies as function of the basis set. Due to the underestimation of the gap, as a consequence of LDA, it is usual to align the conduction band maximum (CBM) with the experimental value, at 1.52 eV from the valence band maximum (VBM). The left panel displays the ionization energies as functions of the basis set for the Ga vacancy that are all below the experimental midgap. The right panel shows the two ionization levels for the As vacancy located below and above the midgap and their convergence with respect to the different basis sets used. Refer to the text for the basis set description.

The use of the Γ point gives only formation energies that are reasonably converged for Ga vacancies. Similarly, the bond lengths around the vacancy and the relaxation volume (Fig. 2) are near those of the 2×2×2, preserving the T_d relaxation symmetry for all charge states.

The use of the Γ point only produces less reliable results in the case of As vacancies. Formations energies are well converged but the relaxation symmetry around the defect is not correctly predicted for all charge states. With the Γ point, the distance between the atoms forming the tetrahedron as well as its associated volume are already converged for charge stated +1, 0, and −1, as shown in Fig. 2.

For V_{As}^{-2}, Γ-point sampling overestimates the volume contraction around the defect by 7.5%. The long bonds in the pairing mode associated with the D_{2d} structure are shortened from 3.46 Å for this sampling to 3.26 Å for 2×2×2 sampling. The k point sampling effect becomes even stronger for the highly charged V_{As}^{-3}. The resonant bond geometry present with high-density sampling (discussed further in Sec. IV B 1) is not found with the Γ-point sampling and the defects relax into the usual pairing mode with two short bonds and four long bonds.

TABLE IV. Convergence of the formation energies E_f' (in eV) for Ga and As vacancies with respect to the Brillouin zone sampling. Percentages refer to the corresponding relative difference in formation energies between the two sampling schemes.

	+1	Neutral	−1	−2	−3
			$E_f'(V_{Ga})$		
Γ		2.51	2.73	3.17	3.81
2×2×2		2.94	3.00	3.40	3.94
		15%	9%	7%	3%
			$E_f'(V_{As})$		
Γ	2.73	3.21	3.52	4.70	6.08
2×2×2	2.79	3.25	3.33	4.52	5.86
	−2%	−1%	6%	4%	4%

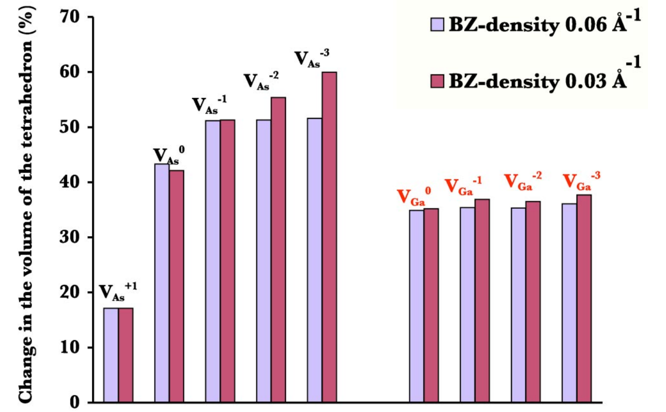

FIG. 2. (Color online) Histogram of the change in the volume of the relaxed tetrahedron formed by atoms surrounding the vacancy in % of the ideal one for two densities of k points in the Brillouin zone (refer to the text for details). For comparison, data for Ga and As vacancies in different charge states are plotted in the same figure.

Comparing the two samplings for V_{As}^{-3}, we find that (1) with the DZP+2^3 mesh, the resonant-bond configuration has the lowest energy; (2) the pairing mode configuration is unstable using the DZP+2^3 mesh, starting from this configuration, the defect relaxes back into the resonant-bond state; (3) for Γ-point sampling the resonant bond configuration is found to be metastable but the pairing mode is favored with an energy difference of 0.6 eV.

Overall, the use of Γ-point sampling gives a reasonable description of the energetic and structural properties of the Ga vacancy as well as most charge states for As. It fails, however, for heavily charged defects, when many electrons are involved in the bonding.

C. Supercell size effects

Size effects on defect formation energies have been widely discussed for a number of systems including the silicon vacancy (see Ref. 22, and references therein) and GaAs.[7] Size effects are found to be strong for cubic supercells smaller than 216±1 atoms for both materials and become negligible for larger systems. For this reason, we will study in this section size effects on charged Ga and As vacancies for supercells of 216 ionic sites and smaller.

To characterize the size effects, we consider the dominant charge state for each vacancy type V_{As}^{-1} and V_{Ga}^{-3}, with the DZP basis set. We simulate two cell sizes with the same k point density: a 63-atom unit cell with a 3×3×3 sampling and a 215-atom cell with 2×2×2 sampling.[7]

We find a formation energy of 3.83 eV compared to 3.33 eV obtained for the 215 cell for V_{As}^{-1}. In this case size effects are strong and overestimate the formation energy by 0.5 eV. More important, the symmetry of the relaxed defect is different for the two sizes: in the 63-atom cell, the defect relaxes to a C_{2v} symmetry while the defect in 215-atom cell adopts a D_{2d} symmetry (Table III). We check that the 63-atom cell is not caught into a metastable state by relaxing the defect starting in a D_{2d} symmetric state. After full relaxation, the cell relaxes into a C_{2v}, confirming that this is the lowest-energy symmetry for this cell. The different symmetry also impacts the change in the volume surrounding the defect. As a consequence of the strong defect-defect interaction in the smaller cell, the structural relaxation is hindered and the volume decreases by 43.8% compared with 51.2% for the 215-atom cell.

As could be expected from the previous sections, size effects are less important for V_{Ga}^{-3}. In particular, the initial tetrahedral symmetry (T_d), with atoms equidistant, is maintained around the defect for the relaxed 215-atom supercell. The same symmetry is found in the 63-atom supercell. Intercell defect-defect interaction rigidifies the lattice, however, and the change in volume is only 34.8% for the 63-atom cell compared to 37.7% for the larger supercell. As with V_{As}^{-1}, the formation energy is overestimated with the small cell: $E_f^{63}=4.24$ eV while $E_f^{215}=3.94$ eV. This difference is considerable as it is on the order of the ionization energies.

D. Summary

In this section, we have studied in details the effects of the choice of basis set, k-point sampling, and simulation cell on the properties of charged defects. In summary, we find that (1) the DZP basis set is well converged and ensures reliable results for all charge states. For a number of charged states, it is also possible to use cheaper optimized basis sets for a similar accuracy. This is not always the case, however, and the applicability of these basis sets must be evaluated on a case by case basis. (2) SZ is less efficient than DZP for defects where symmetry is broken, but it gives a satisfactory estimation of the location of ionization levels in the band gap. (3) For a supercell of 216 atoms or more, the density of k points has only a minor effect on the defect relaxation. The use of the Γ point only gives a relaxation and a symmetry that are satisfactory, in most cases. However, this reduced sampling must be used with care for highly charged defects such as V_{As}^{-3}. (4) The errors arising from size effects are much more important than those coming from the density of k points. In particular, size effects can be the source of errors in estimating the ionization energies, especially when the transition from a charge state to another induces breaking of the symmetry.

IV. DISCUSSION

Here we discuss the results reported in the previous sections; we concentrate on the highly converged results for the Ga and As vacancies, obtained using the DZP basis set, a 215 supercell, and a Monkhorst-pack grid of $2\times2\times2$ in the reciprocal space. We invite the reader to refer to the DZP results reported, in bold, in Tables II and III. We first deal with the stochiometric case where $n_{\mathrm{Ga}}=n_{\mathrm{As}}$ ($\Delta\mu=0$), then we study the formation energies for each kind of defect separately under ideal growing conditions as a function of the doping level. Next, the dominant vacancy type defects in real GaAs crystals are identified by taking into account growing conditions. The ionic chemical potentials vary from As-rich conditions ($\Delta\mu=-\Delta H$) to Ga-rich conditions ($\Delta\mu=+\Delta H$) as the Fermi level is changed progressively.

A. Gallium vacancies

1. Relaxation geometry

Table II describes the fully relaxed geometry of the defect. The structural deformation obtained is well localized around the vacant site; the magnitude of the relaxations is listed for the nearest-neighbor As atoms in all relevant charge states, reaching 15% of the bulk bond distances. The tetrahedral symmetry T_d is always conserved for this defect, irrespective of the charge state: only the breathing mode matters here. The As dangling bonds do not form pairs in any charge state, but the back bonds formed with Ga atoms are clearly weakened; this is in agreement with the observation that the pairing mode is generically not energetically favorable for cation vacancies (Ga).[32] We also observe that all As atoms relax inward but the amount of the relaxation does not increase significantly as more electrons are added to the vacancy levels but remains almost stable (13.5–14.5 %). Our results are in good agreement with the *ab initio* calculations of Laasonen *et al.*[3] and the empirical tight-binding simulations of Seong and Lewis[4] who found a systematic inward relaxation with tetrahedral symmetry for Ga vacancies in the (0,−1,−2) charge state.

2. Energetics

Experimentally, the Ga vacancy is found to exist in the 0,−1,−2,−3 charge states. Until recently, the preferred charge state for the Ga vacancy in GaAs was the subject of a hot debate: most calculations[1,4–6] find that where GaAs in either semi-insulating or n type and Fermi energy is away from the valence band edge, the gallium vacancy is in the triply negative charge, while diffusion experiments suggest a charge of −2 or −1.[33]

Using positron annihilation to determine the Gibbs free energy of formation for Ga vacancies in GaAs, Gebauer *et al.*[34] could finally resolve this debate, giving a quantitative estimation of the formation enthalpy for V_{Ga}^{0} and V_{Ga}^{-3}. The vacancy concentration is directly probed with positron annihilation in Te-doped GaAs as function of doping concentration, temperature, and chemical potential. Our estimate of the formation energies reported in the first column of Table II are in good agreement with recent experimental and theoretical data. For the neutral vacancy, we get $E_f'(V_{\mathrm{Ga}}^{0})=2.94$ eV, a value that agrees with $E_f'(V_{\mathrm{Ga}}^{0})=2.8$ eV from Bockstedte and Scheffler[35] (earlier first-principles calculations[5] predict 3.0 eV) and the experimental results of Gebauer *et al.*[34] $H_f'(V_{\mathrm{Ga}}^{0})=3.2\pm0.5$ eV. A formation enthalpy of 1.8 ± 0.5 eV

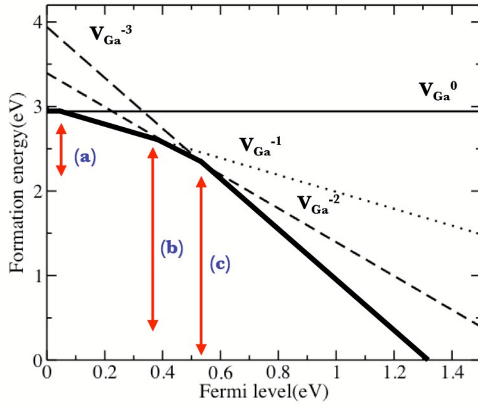

FIG. 3. (Color online) Formation energies as function of Fermi level in various charge states of Ga vacancies at 0 K calculated for stochiometric GaAs ($\Delta\mu=0$). The Fermi level is defined by reference to the valence band maximum. Ionization levels are defined as the intersection between the formation energies of different defects. Defect with the lowest formation energy is dominant. Arrows point to the location of the ionization levels labeled (a) for (0/−), (b) for (−/−2), and (c) for (−2/−3).

was also measured by Mitev *et al.*[36] using interdiffusion experiment on AlGaAs/GaAs heterostructure. However, the charge state of the associated defect is unknown, rendering the comparison with our results difficult.

For the triply negative charge state, we find that $E_f'(V_{\text{Ga}}^{-3})=3.9$ eV. This value compares well with recent experiments[34] which give $H_f'(V_{\text{Ga}}^{-3})=3.6$ eV as well as with recent theoretical study by Janoti *et al.*[8] (3.6 ± 0.2 eV).

Considering the stochiometric case where $n_{\text{Ga}}=n_{\text{As}}$ ($\Delta\mu=0$), we can study the formation energies of GaAs under ideal growing conditions as a function of the doping level. Figure 3 displays the formation energies as a function of Fermi energy for various charge states of Ga vacancies at 0 K. As E_f depends linearly on the electronic chemical potential μ_e, the slope of each of the lines represents the net charge for the system q. Intersections determine the ionization levels where one electron is transferred from the electron reservoir to the defect level. We can see that at each transition only one electron is transferred at a time. Moreover, the ionization levels labeled a, b, and c favor the stability of the −3 charge states for intrinsic and n-type GaAs.

In order to compare with earlier theoretical work, we summarize the results into three types of behavior reported in Table V. (1) Sole among all calculations, Seong and Lewis[4] find a negative-U effect for the Ga vacancy using TB-MD method, the transition levels identified are very shallow and favor the triply negative state in almost the entire range of the Fermi level. (2) The second category of levels reported in Refs. 5–8 are shallow and lie well below the midgap with no negative-U effect detected. (3) Defects level can also lie deeper below the midgap. This is the case for levels a, b, and c in Fig. 3, which compare well with the results of Cheong and Chang[1] and Baraff and Schlüter.[10] Also with a recent study form Gorczyca *et al.*[31] where the −3 charge of V_{Ga} is relevant only if the Fermi energy is above 0.55 eV for arsenic-rich conditions.

Unfortunately, ionization levels cannot be directly measured experimentally, only their sum is obtainable. Nevertheless, experimental values obtained by electron irradiation of GaAs (Ref. 37) support the assignment of deep-lying levels in GaAs, in agreement with the third category. Gebauer *et al.*[34] confirm this assignment using a model to fit their experimental data in order to identify the charge state of the vacancy in GaAs from the location of the ionization levels: using the values for the deep ionization energies obtained by Baraff and Schlüter[10] on unrelaxed Ga vacancies (which are in agrement with our more precies calculations), Gebauer *et al.* show that the −3 charge state is the most stable charge state.

B. Arsenic vacancies

1. Relaxation geometry

As vacancies in various charge states have been studied by a number of authors[3,4,38] taking into consideration ionic

TABLE V. Comparison between ionization energies (measured from the valence band edge) of the Ga vacancy in GaAs. Results are grouped following the three classes discussed in the text.

	Ionization levels (eV)				
				Negative U	
Authors	0/−1	−1/−2	−2/−3	+1/−1	−1/−3
Seong and Lewis (Ref. 4)				0.035	0.078
Northrup and Zhang (Ref. 5)	0.19	0.2	0.32		
Pöykkö *et al.* (Ref. 6)	0.11	0.22	0.33		
Schick *et al.* (Ref. 7)	0.09	0.13	0.20		
Janoti *et al.* (Ref. 8)	0.13	0.15	0.18		
Jansen and Sankey (Ref. 9)	0.1	0.35	0.50		
Baraff and Schlüter (Ref. 10)	0.2	0.5	0.7		
Cheong and Chang (Ref. 1)		0.49	0.69		
Gorczyca *et al.* (Ref. 31)	0.39	0.52	0.78		
This work	0.05	0.4	0.55		

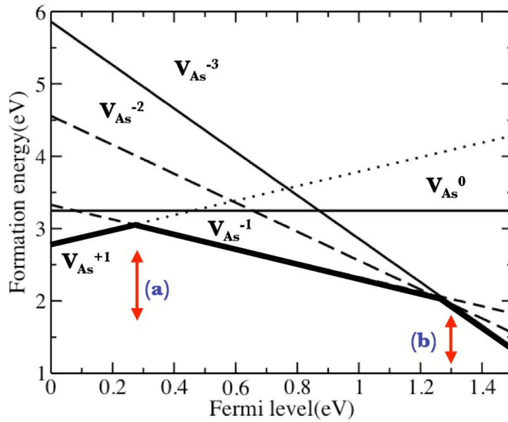

FIG. 4. (Color online) Formation energies as a function of the Fermi energy of various charge states of As vacancies at 0 K. The Fermi level is calculated with respect to the valence band maximum. Arrows point to the location of the ionization levels labeled (a) for (+/−), (b) for (−/−3).

relaxation and relaxation geometry. Except for V_{As}^{+1}, breathing mode displacement breaks the vacancy local symmetry.[3,4] Contrary to Ga vacancy, the volume of the As vacancy increases as electrons are added and shrinks when electrons are removed.

Our results confirm part of these findings. From Table III, the volume of the tetrahedron shrinks from −17 to −60 % of the initial volume as electrons are added to the vacancy. However, all charge states, even positive ones, display inward relaxation with respect to the unrelaxed volume.

Comparing the bond lengths obtained after a full relaxation of the structure (Table III), we find that for the positively charged vacancy (V_{As}^{+1}) there is no electron in the localized states and all four atoms relax inward by about −6% conserving the tetrahedral symmetry, with no Jahn-Teller distortion. Although this inwards relaxation is more important, in absolute value, than the outward relaxation reported in Ref. 3 and 4, they agree in term of the conservation of the symmetry.

For the neutral As vacancy in GaAs (V_{As}^{0}), there is just one electron in the localized state formed by the dangling bonds. The volume reduction is more than twice as large as for the positively charged defect. This change in volume is associated with a Jahn-Teller distortion with the formation of two dimers, leading to two short (–11.5%) and four long Ga—Ga bonds (–24.5%) arranged in a D_{2d} symmetry. This stretches and weakens the back bonds but it allows all atoms to recover a fourfold coordination.

Using *ab initio* molecular dynamics, Laasonen *et al.*[3] see a small (2–3 %) outward relaxation, and an even smaller (0.6%) pairing-mode relaxation, leading to a weak tetragonal distortion with D_{2d} symmetry. This calculation was found to suffer from band dispersion for the localized defect states due to the artificial interaction between unit cells; as a consequence atoms surrounding the vacancy are not allowed to relax properly. Using tight-binding molecular dynamics, a larger breathing-mode displacement was obtained by Seong and Lewis.[4] They find that local tetrahedral symmetry was broken, as one neighbor atom of the defect relaxes inward while the other three relax outward. The pairing mode relaxation is also found to be very small. Feng *et al.*,[38] using a similar method with a 64-atom supercell, found similar results leading to trigonal distortion with C_{3v} symmetry.

TABLE VI. Comparison between ionization energies (measured from the valence band edge) for the As vacancy in GaAs. The data are grouped according to the two categories discussed in the text.

Authors	Ionization levels (eV)			
			Negative U	
	+1/0	0/−1	+1/−1	−1/−3
Seong and Lewis (Ref. 4)	1.41	1.54		
Jansen and Sankey (Ref. 9)	1.30	1.40		
Cheong and Chang (Ref. 1)			0.785	
Pöykkö *et al.* (Ref. 6)			0.86	
This work			0.27	1.27

The difference between our results and previous calculations come from the use of a better converged potential as well as of a larger unit cell. Moreover, as stated previously, we have started the relaxation from various random geometries, always converging to the same final state: the lowest-energy configuration has D_{2d} symmetry for neutral V_{As}.

The extra electron added to get V_{As}^{-1} can be accommodated in the same localized level as the previous one. A stronger pairing mode relaxation appears and the two short bonds become stronger (from –24.5 to –31.5%) atoms of the dimer get closer, while the long bond are almost kept fixed. In agreement with our results reported in Table III, Chadi,[32] using LDA and 32-atom supercell, finds that the −1 charge state arises from a direct transition from the +1 state due to a pairing of the neighboring Ga atoms and has C_{2v} symmetry (pairing mode). The Ga atoms would then move by 0.8 Å (∼−20%) from their ideal position to form two sets of paired bonds.

The next electrons added to the localized levels occupy a different state. The arrangement of the atoms around the doubly negative vacancy V_{As}^{-2} is directly affected: the short bonds remain unchanged but the long bond become stronger passing from −12.6–−17.6 % with a slight change in the relaxation volume. The dimers are therefore brought closer without affecting the intradimer distance.

Most interestingly, the relaxation geometry is modified when a fourth electron is added. In particular, there is an inversion in the Jahn-Teller distortion and the pairs of atoms forming the two dimers get closer to each other and form new weak Ga—Ga bonds with a length equal to the intradimer distance. Finally a tetramer is formed where the four Ga atoms are equidistant and fivefold coordinated (three covalent Ga—As bonds and two weaker Ga—Ga bonds). The tetrahedron formed by the vacancy's first neighbor has four short bonds and two long bonds, as can be clearly seen from Table III.

This type of relaxation, "resonant bond" model, was first seen in calculations for the singly negative divacancy in silicon,[39,40] then for divacancies in GaAs.[6] More recently,

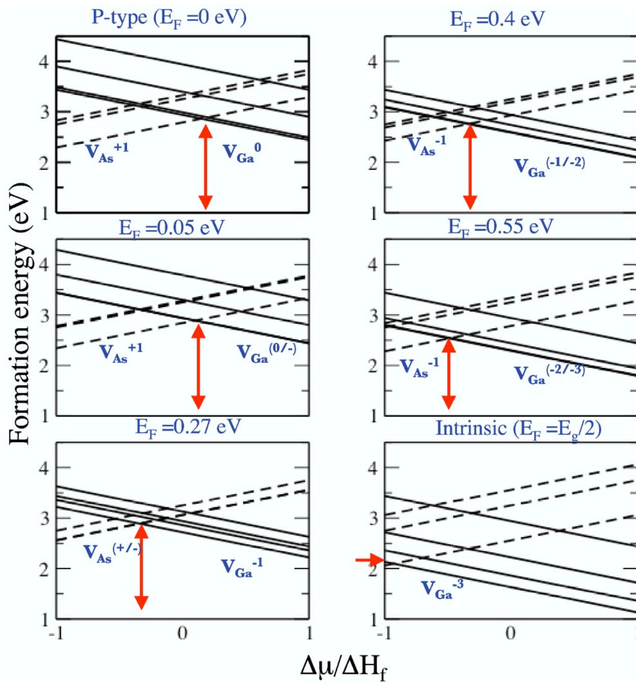

FIG. 5. (Color online) Formation energies of Ga (solid line) and As (dashed line) vacancies in GaAs as a function of the growth conditions ($\Delta\mu$). Different panels are for different critical values of the Fermi level or ionization levels identified earlier.

this relaxation pattern has been observed experimentally, then confirmed using *ab initio* cluster calculations[41] for the $As_{Si}-V_{Si}$ pair in silicon.

2. Energetics

We calculate the formation energies for all possible charge states of the As vacancy; the most relevant defects are reported in the first row of Table IV. Most of the earlier calculations deal with the positively charged vacancy and do not go beyond the −1 charge state; there are no recent calculations that report formation energies for the −2 and −3 charge states.

In a 32-atom supercell LDA calculation for the formation energy of charged defects, Northrup and Zhang find that the outwards relaxed V_{As}^{+3} shows an sp2-like bonding and that it is stable for both intrinsic and *p*-type materials,[42] with a formation energy 1.7 eV lower than the (+1) charge state. Our results are in complete disagreement with this calculation, possibly because of size effects. In the stable geometry, atoms around the defect relax inwards conserving the T_d symmetry. The local volume is decreased by −16.21%. In addition, the corresponding formation energy we obtain does not favor the (+3) charge state under any doping or growing conditions: $E_f'(V_{As}^{+3})=3.5$ eV compared to $E_f'(V_{As}^{+1})=2.8$ eV [in agreement with other calculations: $E_f'(V_{As}^{+1})=2.97$ eV (Ref. 5) using LDA and 3.09 eV (Ref. 43) using self-consistent charge-density-based tight binding]. This confirms that +1 has the lowest energy among all other defects.

Figure 4 displays the formation energies as a function of Fermi level for various charge states of As vacancies at 0 K. For *p*-type GaAs (Fermi level close to the valence band maximum) the +1 charge state has the lowest energy, in agreement with recent results from Chadi.[32]

We note, moreover, that lines for the neutral and the negative charge state intersect before those for the positive and neutral state; the (0/−) ionization level is located well below the (+/0) level and represents a net signature of level inversion or of the so-called negative-U effect.[29] It is therefore energetically more favorable to transfer two electrons at the same time to the defect level from the Fermi level with the reaction $V_{As}^{+}+2e\rightarrow V_{As}^{-}$.

Such a transfer is associated with the strong Jahn-Teller distortion discussed in Sec. IV B 1 as the system goes from the +1 to the −1 state. The negatively charged vacancy remains stable for intrinsic and *n*-type GaAs but is superseded by the triply negative vacancy in the heavily *n*-doped GaAs corresponding to $E_F=1.27$ eV (level *b* in Fig. 4): the (−/−2) and (−2/−3) defect levels almost collapse, thus the direct (−/−3) transition is favored. Interestingly, the transition (−/−3) is associated with a structural change from the pairing mode relaxation to the resonant mode relaxation as discussed in Sec. IV B 1. The four added electrons are paired two by two as the energy gained from the structural relaxation overcomes the Coulombic repulsion for each of the two electrons, supplying a net effective attractive interaction between the electrons.

Only the +1, 0, and −1 charge states seem to have been studied previously by *ab initio* calculations. While Northrup and Zhang[5] predict that arsenic vacancy in GaAs exists in the + charge state only, other calculated ionization levels split into two main categories classified in Table VI: (i) a direct transition from a charge state to another is possible with only one electron transferred at a time and (ii) a negative-U effect for the (+/−) transition. The first type of transition was found by Seong and Lewis,[4] who predict V_{As} to exist only in the + charge state, at 1.41 eV above the valence band this charge state changes to neutral then to negative charge state at the limit of the conduction band maximum. In an earlier study for unrelaxed As vacancies reported by Jansen and Sankey[9] ionization energies are located in the range of experimental band gap and located near the conduction band maximum. A negative-U effect is reported by both Cheong and Chang[1] and Pöykkö *et al.*[6] for the (+/−) transition, the transfer of the two electron occurs above the middle of the band gap. This negative-U behavior is confirmed by a recent calculation from Chadi,[32] who finds that the direct transition $V_{As}^{+}+2e\rightarrow V_{As}^{-}$ is favored after a Jahn-Teller distortion and that −1 charge state is the most stable for Fermi levels above midgap.

Our results agree partially with these results. There is a negative-U effect but the level for the (+/−) transition is shallower. This might be due to the important structural relaxation that affects the neutral and negatively charged vacancies. Moreover, as discussed above, we also find a second negative-U transition level at $E_F=1.27$ eV with the reaction $V_{As}^{-}+2e\rightarrow V_{As}^{-3}$.

Real GaAs crystals are far from being perfectly stochiometric; during growth there will be an excess of Ga or As ions. A more general study concerns the effect of the grow-

ing conditions on the stability of the defect under certain doping conditions. In Fig. 5, the various panels show the progressive doping of the GaAs sample and how the stability of the defect gets consequently affected. The Fermi level ranges between the valence band maximum and the midgap where most of the ionization levels computed in this work have been identified. Each of the panels shows the transition between two charge states for As and Ga vacancies at the critical values of the ionization levels. For example, at $E_F=0.05$ eV the first transition for gallium vacancies takes place, the two lines collapse and are indicated as $V_{\mathrm{Ga}}^{(0/-1)}$.

For p-type GaAs, at the As-rich limit in GaAs, corresponding to $\Delta\mu/\Delta H_f$ close to -1, the dominant charge state is the As vacancies that probably compete with As antisites, while for the Ga-rich limit Ga vacancies have lower formation energies. For a Fermi energy at midgap and for n-type GaAs, regardless of the growing condition, the triply negative charge state is the most stable among others and has the lowest formation energy.

V. CONCLUSIONS

We have presented a complete description of the energetic and the relaxation geometry for relevant vacancy-type defects in GaAs using the SIESTA *ab initio* program. Various convergence tests show that size effects, the completeness of the basis sets, and the sampling of the Brillouin zone can become very important when the symmetry of the defect is broken or when the defect is highly charged.

Using the DZP basis set, with a 216-atom unit cell and a $2\times2\times2$ k-point sampling, we find that Ga vacancies have shallow ionization levels below midgap in agreement with experiment, and do not show any recombination of the dangling bonds as was shown in an earlier calculation.[3,4] For the less studied As vacancy, we find that the ionization level $(+/-)$ of As is located in the lower half of the band gap and lies near the valence band while the second negative-U level $(-/-3)$ is located above midgap with a significant difference in the relaxation pattern reported earlier. The triply negative charge state for As vacancy reconstruct in the resonant bond mode, in a similar fashion as divacancies in Si and GaAs reported earlier. Finally, we find that only a few vacancy types can act as vehicles for self-diffusion of dopants in real GaAs devices under different doping and growing conditions, such as the triply negative Ga vacancy for intrinsic and n-type GaAs. These results will be used as a starting point for a detailed study of self-diffusion using the SIEST-A-RT method presented elsewhere.[21]

ACKNOWLEDGMENTS

We thank Pablo Ordejón for his help in the initial optimization of the basis sets. This work was funded in part by NSERC, FQRNT, and the Research Canada Chair program. N.M. was supported by a Cottrell Research Corporation Scholarship. Most of the simulations were run on the computers of the Réseau québécois de calcul de haute performance (RQCHP) whose support is gratefully acknowledged.

*Electronic address: f.el.mellouhi@umontreal.ca
†Electronic address: Normand.Mousseau@umontreal.ca

[1] B.-H. Cheong and K. J. Chang, Phys. Rev. B **49**, 17 436 (1994).
[2] S. B. Zhang and J. E. Northrup, Phys. Rev. Lett. **67**, 2339 (1991).
[3] K. Laasonen, R. M. Nieminen, and M. J. Puska, Phys. Rev. B **45**, 4122 (1992).
[4] H. Seong and L. J. Lewis, Phys. Rev. B **52**, 5675 (1995).
[5] J. E. Northrup and S. B. Zhang, Phys. Rev. B **47**, 6791 (1993).
[6] S. Pöykkö, M. J. Puska, and R. M. Nieminen, Phys. Rev. B **53**, 3813 (1996).
[7] J. T. Schick, C. G. Morgan, and P. Papoulias, Phys. Rev. B **66**, 195302 (2002).
[8] A. Janotti, S.-H. Wei, S. B. Zhang, and S. Kurtz, Phys. Rev. B **67**, 161201 (2003).
[9] R. W. Jansen and O. F. Sankey, Phys. Rev. B **39**, 3192 (1989).
[10] G. A. Baraff and M. Schlüter, Phys. Rev. Lett. **55**, 1327 (1985).
[11] Deepak D. Balamurugan, and K. Nandi, Bull. Mater. Sci. **1**, 169 (2003).
[12] D. Sánchez-Portal, P. Ordejón, E. Artacho, and J. M. Soler, Int. J. Quantum Chem. **65**, 453 (1997).
[13] J. M. Soler, E. Artacho, J. Gale, A. García, J. Junquera, and P. Ordejón, J. Phys.: Condens. Matter **14**, 2745 (2002).
[14] N. Troullier and J. L. Martins, Phys. Rev. B **43**, 1993 (1991).
[15] L. Kleiman and D. M. Bylander, Phys. Rev. Lett. **48**, 1425 (1982).
[16] J. Junquera, O. Paz, D. Sánchez-Portal, and E. Artacho, Phys. Rev. B **64**, 235111 (2001).
[17] E. Anglada, J. M. Soler, J. Junquera, and E. Artacho, Phys. Rev. B **66**, 205101 (2002).
[18] G. Zolo and R. M. Nieminen, J. Phys.: Condens. Matter **15**, 843 (2003).
[19] *Handbook Series on Semiconductor Parameters*, edited by M. Levinshtein, S. Rumyantsev, and M. Shur (World Scientific, London, 1996), Vol. 1.
[20] *Handbook of Chemistry and Physics*, edited by C. Weast, 73rd ed. (CRC, Boca Raton, FL, 1992).
[21] F. El-Mellouhi and N. Mousseau (unpublished).
[22] F. El-Mellouhi, N. Mousseau, and P. Ordejón, Phys. Rev. B **70**, 205202 (2004).
[23] M. I. J. Probert and M. C. Payne, Phys. Rev. B **67**, 075204 (2003).
[24] L. Torpo, M. Marlo, T. E. M. Staab, and R. M. Nieminen, J. Phys.: Condens. Matter **13**, 6203 (2001).
[25] S. B. Zhang and A. Zunger, Phys. Rev. Lett. **77**, 119 (1996).
[26] G. Makov and M. C. Payne, Phys. Rev. B **51**, 4014 (1995).
[27] M. Bockstedte, A. Mattausch, and O. Pankratov, Phys. Rev. B **68**, 205201 (2003).
[28] J. Lento, J. L. Mozos, and R. M. Nieminen, J. Phys.: Condens. Matter **14**, 2637 (2002).
[29] P. W. Anderson, Phys. Rev. Lett. **34**, 953 (1975).
[30] H. J. Monkhorst and J. D. Pack, Phys. Rev. B **13**, 5188 (1976).
[31] I. Gorczyca, N. E. Christensen, and A. Svane, Phys. Rev. B **66**,

075210 (2002).
[32] D. J. Chadi, Mater. Sci. Semicond. Process. **6**, 281 (2003).
[33] B. Bracht, E. E. Haller, K. Eberl, and M. Cardona, Appl. Phys. Lett. **74**, 49 (1999).
[34] J. Gebauer, M. Lausmann, F. Redmann, R. Krause-Rehberg, H. S. Leipner, E. R. Weber, and P. Ebert, Phys. Rev. B **67**, 235207 (2003).
[35] M. Bockstedte and M. Scheffler, Z. Phys. Chem. (Munich) **200**, 195 (1997).
[36] P. Mitev, S. Seshadri, L. J. Guido, D. T. Schaafsma, and D. H. Christensen, Appl. Phys. Lett. **73**, 3718 (1998).
[37] Q. Y. Jia, H. J. von Bardeleben, D. Stienvard, and C. Delerue, Phys. Rev. B **45**, 1645 (1992).
[38] Y. P. Feng, C. K. Ong, H. C. Poon, and D. Tománek, J. Phys.: Condens. Matter **9**, 4345 (1997).
[39] M. Saito and A. Oshiyama, Phys. Rev. Lett. **73**, 866 (1994).
[40] H. Seong and L. J. Lewis, Phys. Rev. B **53**, 9791 (1996).
[41] S. Öğüt and J. R. Chelikowsky, Phys. Rev. Lett. **91**, 235503 (2003).
[42] J. E. Northrup and S. B. Zhang, Phys. Rev. B **50**, 4962 (1994).
[43] T. E. M. Staab, M. Haugk, T. Frauenheim, and H. S. Leipner, Phys. Rev. Lett. **83**, 5519 (1999).